

1-1-2003

# A Stibonium-Modified Clay and its Polystyrene Nanocomposite

Dongyan Wang  
*Marquette University*

Charles A. Wilkie  
*Marquette University, [charles.wilkie@marquette.edu](mailto:charles.wilkie@marquette.edu)*

Marquette University

e-Publications@Marquette

***Chemistry Faculty Research and Publications/College of Arts and Sciences***

***This paper is NOT THE PUBLISHED VERSION; but the author's final, peer-reviewed manuscript. The published version may be accessed by following the link in the citation below.***

*Journal/Monograph*, Vol. xx, No. x (xxxx): XX-XX. [DOI](#). This article is © [publisher] and permission has been granted for this version to appear in [e-Publications@Marquette](#). [publisher] does not grant permission for this article to be further copied/distributed or hosted elsewhere without the express permission from [publisher].

# A Stibonium-modified Clay and Its Polystyrene Nanocomposite

Dongyan Wang

Department of Chemistry, Marquette University, Milwaukee, WI

Charles A. Wilkie

Department of Chemistry, Marquette University, Milwaukee, WI

## Abstract

Triphenylhexadecylstibonium trifluoromethylsulfonate has been prepared and ion-exchanged with sodium montmorillonite to obtain a new organically-modified clay. The clay has higher thermal stability than an ammonium clay; only a portion of the alkyl chain is lost during degradation and all of the antimony is retained. This clay has been used to prepare a polystyrene nanocomposite in which the clay is not uniformly distributed throughout the polymer. Nonetheless the polymer does insert into the clay layers and the *d*-spacing of the clay expands from 2.0 to 3.0 nm. The enhanced thermal stability of this system may mean that it could be useful for polymers which must be processed at temperatures above that at which the ammonium clays undergo degradation.

## Keywords

Nanocomposite, Polystyrene, Antimony,

# 1. Introduction

The investigation of polymer clay nanocomposites is one of the most active research fields in polymer and materials science in the past decade [\[1\]](#), [\[2\]](#), [\[3\]](#). These materials are of interest because of the enhanced mechanical and thermal properties and due to the decrease in permeability. The combination of a nano-dimensional material with a polymer may yield either an immiscible material, in which the clay is acting as a filler and is not dispersed at the nanometer level, or a nanocomposite may be obtained. If the registry between the clay layers is maintained, the material is described as intercalated, while, if this registry is lost, the material is called exfoliated, also known as delaminated. Nanocomposites may be prepared either by a blending process or by bulk polymerization. Melt blending can be one of the most useful processes, but sometimes high temperatures are required, for instance with a polymer such as polycarbonate. It is expected that this will be the method of choice for most industrial applications [\[4\]](#), [\[5\]](#), [\[6\]](#). Solution blending has also been utilized, especially for materials whose decomposition temperature is lower than its melt temperature, or thermosetting materials that can not be melt processed [\[7\]](#), [\[8\]](#). Solution blending may also provide a better way to obtain finely dispersed clay particles than melt blending. Bulk or in situ polymerization has also been used and frequently this offers better dispersion of the clay than can be obtained by a blending process [\[9\]](#). This perhaps occurs because the monomer is inserted into the gallery space of the clay where it undergoes polymerization giving intercalated or exfoliated polymer clay nanocomposites [\[10\]](#).

Clay contains layered silicate sheets, on which there resides a negative charge, and this is balanced by the charge on cations, typically sodium cations, within the gallery space; thus the gallery space is quite hydrophilic. Polymers and solvents which exhibits hydrophilic properties, such as poly(tetrahydrofuran) (THF) [\[11\]](#), thiophene [\[12\]](#), epoxy [\[13\]](#), poly(vinyl chloride) (PVC) [\[4\]](#), [\[5\]](#), poly(ethylene oxide) (PEO) [\[8\]](#) etc., can directly insert into the gallery space of the natural-occurring clay and may form an intercalated or exfoliated nanocomposite. For the majority of polymers, owing to their hydrophobic character, the clay must be modified with a surfactant in order to make the gallery space sufficiently hydrophobic to permit it to interact with the polymer. The surfactant is usually described as an 'onium' salt, but in fact ammonium salts are most commonly used. These 'onium' salts may have a variety of functionalities that can affect the extent of intercalation or exfoliation [\[14\]](#), [\[15\]](#).

The onset temperature of the degradation of a phosphonium modified clay is about 50 °C higher than that of an ammonium clay [\[14\]](#) and this difference could be important in the melt blending of some polymers. In this study we investigate the preparation and characterization of an antimony-containing clay and the preparation of polystyrene nanocomposites from this clay. The objective of this study is to determine if this clay is more thermally stable than the common ammonium clays and thus could be used at higher temperatures for the processing of polymers, such as polycarbonate, that require processing at higher temperature.

## 2. Experimental

### 2.1. Materials

The majority of chemicals, including monomeric styrene, benzoyl peroxide (BPO) (97%), triphenyl antimony (99%), 1-hexadecanol, trifluoromethanesulfonic anhydride (98+%), and dimethylsulfoxide (DMSO), were acquired from the Aldrich Chemicals Company, Inc. The inhibitor was removed from the monomer by passing it through an inhibitor remover column, also acquired from Aldrich. The sodium clay, Cloisite Na, was a gift from Southern Clay Company, the cation exchange capacity (CEC) was about 92 meq/100 g. All materials were used as received, except monomeric styrene. Distilled water was used throughout.

### 2.2. Synthesis of triphenylhexadecylstibonium trifluoromethylsulfonate

In a 250 ml round bottom flask was added 8.0 g (33 mmol) of 1-hexadecanol in 100 ml DMSO, then 10 g (35 mmol) of trifluoromethanesulfonic anhydride was added drop wise under vigorous magnetic stirring in 5 min.

The solution was magnetically stirred for several hours, and then the volatiles were removed under vacuum, yielding a yellowish viscous solid. A known amount of the hexadecyltrifluoromethane sulfonate (5.0 g, 13 mmol) was transferred to another 250 ml flask with 100 ml of DMSO. To this was added 5.0 g (14 mmol) triphenylantimony and this solution was stirred at room temperature for 1 h, then heated and maintained at 80 °C for 24 h. Finally the solution was cooled and stirred at room temperature for an additional several hours. The solvent was evaporated under vacuum, leaving a colorless solid. MP, 241–243 °C; <sup>1</sup>H NMR (CDCl<sub>3</sub>): δ 7.55–7.33 (*m*, 15H), 3.43–3.39 (*t*, *J*=6.9 Hz, 2H), 1.90–1.81 (*m*, 2H), 1.55–1.26 (*br*, 26H), 0.90–0.86 (*t*, *J*=6.5 Hz, 3H).

### 2.3. Preparation of the organically-modified clay

The organically-modified clay was obtained by treatment of sodium montmorillonite with the stibonium salt using chemistry similar to that previously described for ammonium and phosphonium clays [14], [15]. The sodium clay was dispersed in water for 24 h with vigorous magnetic stirring, at a concentration of about 10% (w/w). Then the predetermined amount of the stibonium salt was added; a precipitate was immediately produced, and the solution was stirred overnight. The amount of stibonium salt is determined by the CEC of the clay and a 10% excess of the stibonium salt was used.

### 2.4. Synthesis of polystyrene nanocomposites

The nanocomposites were prepared by bulk polymerization using the procedure that has been previously reported [16].

### 2.5. Instrumentation

X-ray diffraction (XRD) patterns were obtained using a Rigaku Geiger Flex, 2-circle powder diffractometer equipped with CuK $\alpha$  generator ( $\lambda$ =1.5404 Å). Generator tension is 50 KV and generator current is 20 mA. A Jeol 1200EX transmission electron microscope (TEM) operating at 120 kV was used in this study; the thin sections were microtomed at room temperature and then transferred from the knife-edge to 600 hexagonal mesh Cu grids. The contrast between the layered silicates and the polymer phase was sufficient for imaging, so no heavy metal staining of sections prior to imaging is required. Thermogravimetric analysis (TGA) was performed on Cahn TG131 unit under a 30 ml/min flowing nitrogen atmosphere at a scan rate of 10 °C/min from 20 to 600 °C; temperatures are reproducible to  $\pm 3$  °C and the fraction of non-volatile material is reproducible to  $\pm 3\%$ . Thermogravimetric Analysis Fourier Transform Infrared spectrometry (TGA–FTIR) was obtained on Cahn TG131 unit coupled to a Mattson Research FTIR spectrometer under a 80 ml/min flowing nitrogen atmosphere at a scan rate of 20 °C/min from room temperature to 250 °C and then at a scan rate of 10 °C/min to 600 °C. NMR spectra were obtained on a Varian Mercury300 instrument.

Cone calorimetry was performed on an Atlas CONE-2 according to ASTM E 1354–92 at an incident flux of 35 kW/m<sup>2</sup> using a cone shaped heater. Exhaust flow was set at 24 l/s and the spark was continuous until the sample ignited. Cone samples were prepared by compression molding the sample (about 30 g) into square plaques. Typical results from Cone calorimetry are reproducible to about  $\pm 10\%$ . These uncertainties are based on many runs in which thousands of samples have been combusted [17].

## 3. Results and discussion

The stibonium salt contains one long chain (16 carbon), three phenyl groups and is referred to herein as SbC16; its structure is shown in Fig. 1.

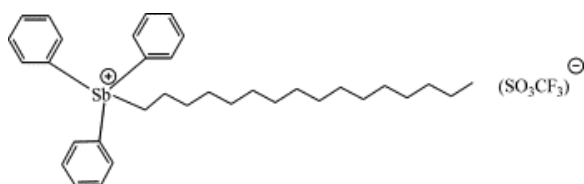


Fig. 1. Structure of triphenylhexadecylstibonium trifluoromethylsulfonate.

### 3.1. X-ray diffraction

X-ray diffraction (XRD) was used to characterize the layered structure of polymer-clay nanocomposites, since changes in  $2\theta$  indicate changes in the gallery height of the clay. [Fig. 2](#) shows the XRD results for the SbC16 modified clay and bulk polymerized styrene with SbC16 clay nanocomposite. The clay shows a strong peak at  $4.5^\circ$  ( $d$ -spacing=2.0 nm) and the peak moves to  $2.9^\circ$  ( $d$ -spacing=3.0 nm) in the nanocomposites obtained upon bulk polymerization. This data suggests the formation of an intercalated structure.

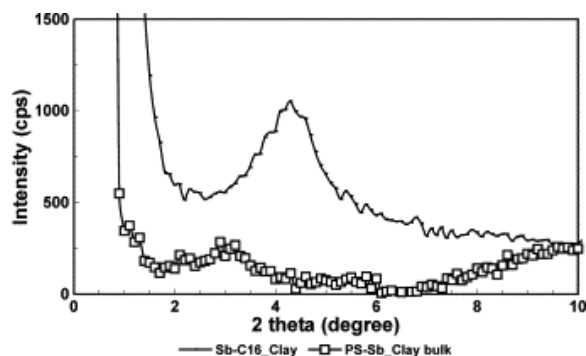


Fig. 2. XRD pattern for the stibonium clay and its corresponding polystyrene nanocomposites; the curves are offset vertically.

### 3.2. Transmission electron microscopy

TEM images have been obtained for the SbC16 clay nanocomposites at a variety of magnifications. At the lowest magnification, shown in [Fig. 3a](#), one can see that the clay is not uniformly distributed throughout the polymer, suggesting that there is some amount of immiscible character to this nanocomposite. At higher magnification ([Fig. 3b](#)), one can clearly see that the clay layers have expanded and that an intercalated material is produced. At the highest magnification ([Fig. 3c](#)), one can see that the interlayer spacing is in the range 3–4 nm, in agreement with the XRD result; there is some suggestion of a small amount of exfoliation.

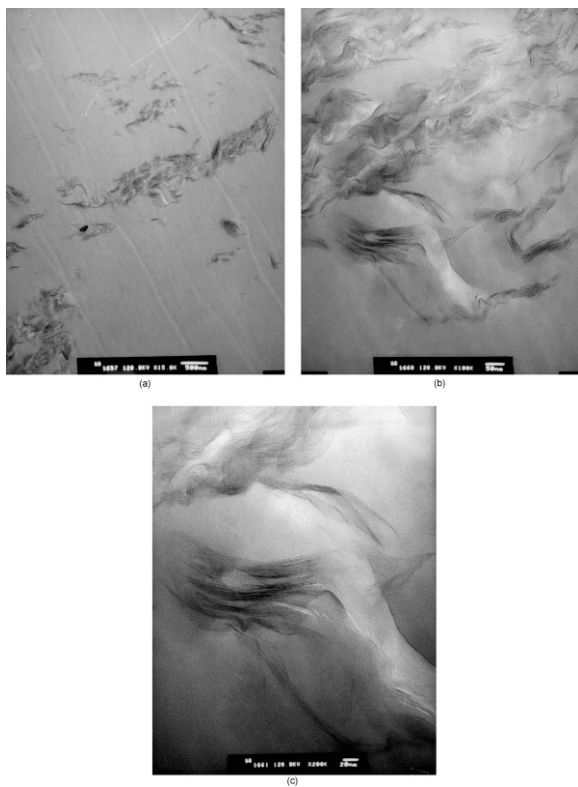


Fig. 3. (a) TEM image of SbC16 PS nanocomposite at low magnification. (b) TEM image of SbC16 PS nanocomposite at higher magnification. (c) TEM image of SbC16 PS nanocomposite at highest magnification.

### 3.3. Thermogravimetric analysis (TGA)

[Fig. 4](#) shows the TGA results for the stibonium clay compared with three typical ammonium clays. VB16 [\[14\]](#) is an ammonium salt which contains one carbon 16 long chain, two methyl groups and one vinyl benzyl group. Cloisite 10A contains two methyl groups, one hydrogenated tallow (~65% C18, ~30% C16, ~5% C14) and one benzyl group, while Cloisite 6A contains two methyl and two hydrogenated tallows. The degradation of the typical ammonium clay occurs in two steps [\[14\]](#), [\[18\]](#). In the first step, which occurs in the range 200–400 °C, the long chain is lost as an olefin and a hydrogen replaces the alkyl group. In the second step, which commences at about 400 °C, the amine is lost and a proton is now the counterion for the clay. In [Fig. 4](#) one can clearly see two steps in the degradation of VB16 and in Cloisite 10A while the degradation of Cloisite 6A appears to occur in only a single step which bridges both temperature regions. The hexadecyl group is 35% of the total mass of the stibonium cation and only 13% of the mass is lost at 400 °C so complete degradation of this cation does not occur, unlike the case of ammonium clays where the degradation is complete. Even at 600 °C for the stibonium cation the mass loss is only 20% and the mass fraction attributable to the cation is greater than in an ammonium clay.

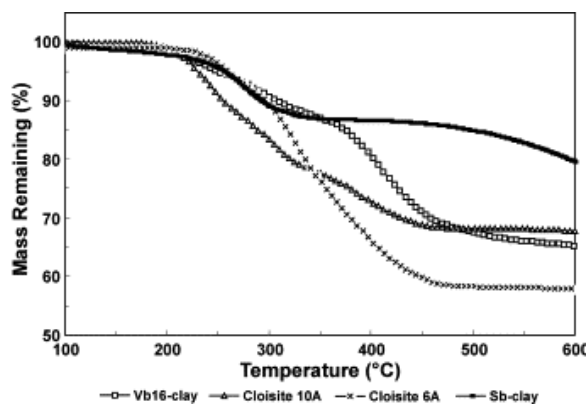


Fig. 4. Comparison of the TGA curves for the stibonium and three ammonium clays.

TGA curves have also been obtained for the polystyrene nanocomposites and this is shown in Fig. 5, together with the curve of polystyrene for comparison. The enhanced thermal stability of the nanocomposite is obvious. The onset temperature of the degradation, as measured by the temperature at which 10% mass is lost, is increased by 50 °C and the mid-point of the degradation is also 50 °C higher for the nanocomposite than for virgin polystyrene. The thermal stability of the polystyrene nanocomposite is quite comparable to what is observed for ammonium clay nanocomposites.

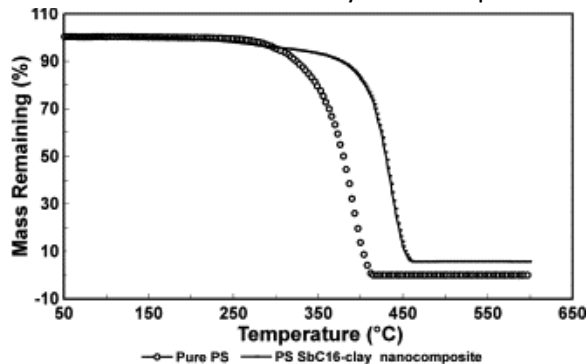


Fig. 5. TGA curves for polystyrene and the stibonium clay polystyrene nanocomposite.

### 3.4. Thermogravimetric analysis—Fourier transform infrared spectroscopy (TGA–FTIR)

TGA–FTIR was utilized to characterize the volatile components that evolve during the degradation of the clay. The spectra that are obtained from the volatiles that evolve from the clay alone are shown in Fig. 6. At 150 °C a very small amount of residual water evolves. As the temperature is increased to 280 °C one can observe a variety of new peaks that are shown in the figure; all peaks, except that at  $1789\text{ cm}^{-1}$  may be attributable to aliphatic C–H vibrations and are due to the loss of hexadecane. The peak in the carbonyl region has been observed before in TGA–FTIR studies [14], [18] and this has been attributed to the formation of either an aldehyde or a ketone. The intensities of the evolved gases decrease as the temperature is increased but the identity of the bands do not change; degradation of the clay continues but no aromatic is lost. The boiling point of triphenylantimony is 377 °C so one would see aromatic absorptions if it did evolve. It is of interest to note that the spectrum obtained at 504 °C shows only very little absorption, much less than what is seen at 403 °C. This means that the degradation of the clay is largely finished before about 500 °C.

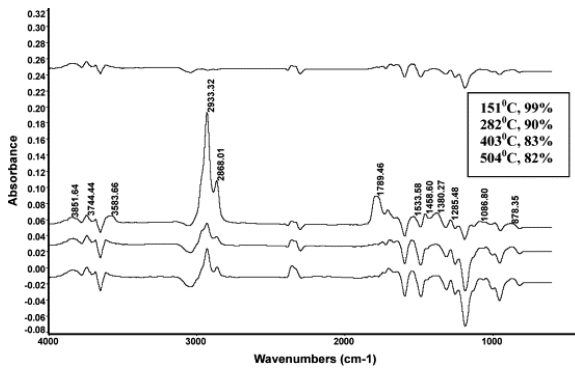


Fig. 6. Spectra of gases that are evolved during the thermal degradation of the stibonium clay at different temperatures. The legend shows the temperature at which the gas evolves and the fraction of the material which has not yet volatilized.

A sample of the clay has been heated to 350 °C and the residue recovered. The presence of both aliphatic and aromatic C–H vibrations are obvious and this is a clear indication that there is still a stibonium salt present in the clay at this temperature; this spectrum is shown in [Fig. 7](#).

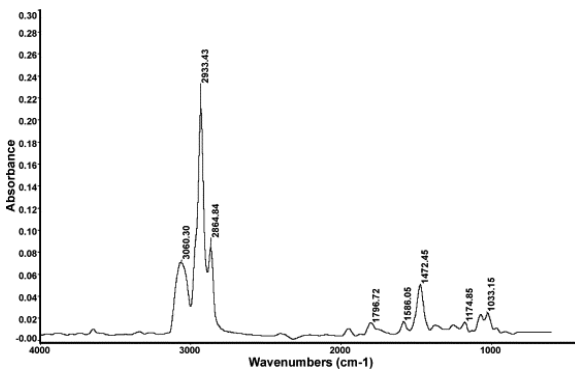


Fig. 7. Infrared spectrum of the residue from thermal degradation of the stibonium clay at 350 °C.

The TGA–FTIR data for the stibonium clay–polystyrene nanocomposite is shown in [Fig. 8](#). At 286 °C there is a very small amount of thermal degradation, as shown by the very weak peaks in the C–H stretching region. At 366 °C this becomes a little more pronounced but the temperature must rise to 428 °C before strong peaks are evident and these are clearly due to aromatic materials, indicating that the degradation of polystyrene is occurring. The same peaks are still evident at 450 °C.

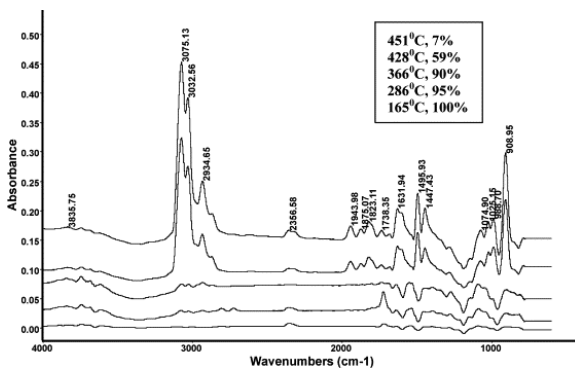


Fig. 8. IR spectra of the volatiles that evolve when a sample of stibonium clay–polystyrene nanocomposite is thermally degraded.

### 3.5. Cone calorimetry

[Table 1](#) shows the cone calorimetric results for the stibonium clay–polystyrene nanocomposite as well as for polystyrene. It is normal for nanocomposites to ignite at an earlier time than does the virgin polymer and this is no exception. The peak heat release rate, PHRR, is decreased by about 20%, the plots of heat release rate as a function of time for both the polymer and its nanocomposite with the stibonium clay are shown in [Fig. 9](#). For polystyrene the best reduction in PHRR that has been observed is about 48% [\[14\]](#). This reduction is not so large and this is likely a reflection that the clay is not uniformly distributed, i.e., there is some microcomposite character to this material.

Table 1. Cone calorimetric data for polystyrene and the stibonium clay–polystyrene nanocomposite

Composition	PS	PS-Sb
Time to ignition, s	51	26
PHRR <sup>a</sup> , kw/m <sup>2</sup>	1381	1111(20%)
Time to PHRR <sup>a</sup> , s	67	88
Time to burn out, s	189	141
Average HRR <sup>b</sup> , kw/m <sup>2</sup>	727	691
Total heat released, MJ/m <sup>2</sup>	92	81
Mass loss rate, g/s *m <sup>2</sup>	13.9	18.4
Average specific ext area, m <sup>2</sup> /kg	1218	1220

aPeak heat release rate.

bHeat release rate.

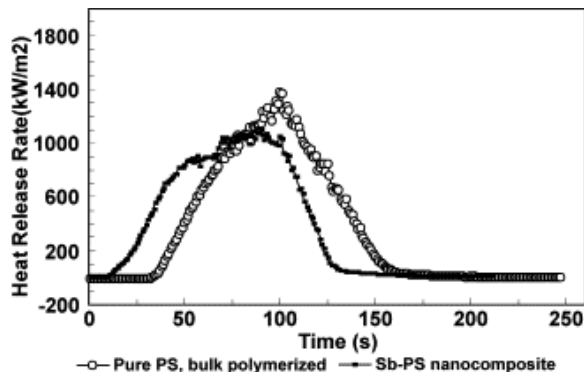


Fig. 9. Heat release rates of Sb-Clay-PS nanocomposite and pure PS.

### 4. Conclusions

A new organically-modified clay has been made with enhanced thermal stability. This antimony-containing clay loses only 20% of its mass by 600 °C, compared to the typical ammonium clay which shows a 30–40% mass loss. By bulk polymerization the clay is not uniformly distributed throughout the polymer matrix so it does show some of the characteristics of a microcomposite. Polymer does insert between the clay layers and there is also evidence of a small amount of exfoliation of the clay. The enhanced thermal stability of this clay may make it useful for polymers which must be processed at temperatures which are above the degradation temperature of the ammonium clays.

## Acknowledgments

This work was performed under the sponsorship of the US Department of Commerce, National Institute of Standards and Technology, Grant Number 70NANB6D0119.

## References

- [1] E.P. Giannelis, R. Krishnamoorti, R. Manias. *Advances in Polymer Science*, 138 (1999), pp. 107-147
- [2] A. Alexandre, P. Dubois. *Materials Science and Engineering*, 28 (2000), pp. 1-63
- [3] T.J. Pinnavaia, G.W. Beall. **Polymer-clay Nanocomposites**. Wiley, New York (2001)
- [4] D. Wang, D. Parlow, Q. Yao, C.A. Wilkie. *J. Vinyl Add. Technol*, 7 (2001), pp. 203-213
- [5] Wang D, Parlow D, Yao Q, Wilkie CA. *J Vinyl Add Technol* 2002;8:139–50.
- [6] R.A. Vaia, E.P. Giannelis. *Macromolecules*, 30 (1997), pp. 8000-8009
- [7] D.J. Greenland. *J. Colloid Sci.*, 18 (1963), pp. 647-664
- [8] N. Ogata, S. Kawakage, T. Ogihara. *J. Appl. Polym. Sci.*, 66 (1967), pp. 573-581
- [9] Wang D, Zhu J, Yao Q, Wilkie CA. *Chem Mater* 2002;14:3837–43.
- [10] Y. Kojima, A. Usuki, M. Kawasumin, A. Okada, Y. Fukushima, T. Karauchi, O. Kamigaito. *J. Mater. Res.*, 6 (1993), pp. 1195-1198
- [11] C.O. Oriakhi, M.M. Lerner. *Mater. Res. Bull*, 30 (1995), p. 723
- [12] H. Nakajima, G.M. Ubayashi. *J. Mater. Chem.*, 5 (1995), p. 105
- [13] T. Lan, T.J. Pinnavaia. *Chem. Mater.*, 6 (1994), p. 573
- [14] J. Zhu, A.B. Morgan, F.J. Lamelas, C.A. Wilkie. *Chem. Mater.*, 13 (2001), pp. 3774-3780
- [15] J. Zhu, P. Start, K.A. Mauritz, C.A. Wilkie. *J. Polym. Sci.: Part A: Polym. Chem.*, 40 (2002), pp. 1498-1503
- [16] J. Zhu, C.A. Wilkie. *Polym. Int*, 49 (2000), pp. 1158-1163
- [17]. J.W. Gilman, T. Kashiwagi, M. Nyden, J.E.T. Brown, C.L. Jackson, S. Lomakin, et al. S. Al-Maliaka, A. Golovoy, C.A. Wilkie (Eds.), *Chemistry and technology of polymer additives*, Blackwell Scientific, London (1998), pp. 249-265
- [18] W. Xie, Z. Gao, W.-P. Pan, R. Vaia, D. Hunter, A. Singh. *Polym. Mater. Sci. Eng.*, 83 (2000), p. 284